



Special issue in honor of Prof. Győző Garab

Single-cell microfluidics in combination with chlorophyll *a* fluorescence measurements to assess the lifetime of the *Chlamydomonas* PSBO protein

E. SZÉLES^{*,***}, S. KUNTAM^{*}, A. VIDAL-MEIRELES^{*}, V. NAGY^{*}, K. NAGY^{***}, Á. ÁBRAHÁM^{***,†}, L. KOVÁCS^{*}, and S.Z. TÓTH^{*,+ }

Institute of Plant Biology, Biological Research Centre, Szeged, H-6726 Szeged, Hungary^{*}

Doctoral School of Biology, University of Szeged, H-6722 Szeged, Hungary^{**}

Institute of Biophysics, Biological Research Centre, Szeged, H-6726 Szeged, Hungary^{***}

Doctoral School of Multidisciplinary Medical Sciences, University of Szeged, H-6720 Szeged, Hungary[#]

Abstract

PSBO is an essential subunit of the oxygen-evolving complex and we recently demonstrated that its lifetime depends on environmental conditions in *Chlamydomonas reinhardtii*. To assess PSBO lifetime with a high time resolution, we employed (1) a microfluidic platform enabling the trapping of single cells and the parallel measurement of photosynthetic activity, and (2) a nitrate-inducible PSBO amiRNA line. Our microfluidic platform allowed the rapid replacement of the nutrient solution necessary for induction. It also enabled the precise monitoring of the decline in the F_v/F_m value, reflecting PSBO loss. We found that in the dark, at medium and high light intensity, the F_v/F_m value decreased with halftimes of about 25, 12.5, and 5 h, respectively. We also observed that photosynthetic activity was better sustained upon carbon limitation. In the absence of acetate, the halftimes of F_v/F_m diminishment doubled to quadrupled compared with the control, acetate-supplied cultures.

Keywords: carbon availability; chlorophyll fluorescence; oxygen-evolving complex; photoinhibition; protein lifetime.

Introduction

In a light-driven cycle, the manganese cluster (Mn_4CaO_5) of photosystem II (PSII) splits water molecules into oxygen, protons, and electrons. In plants and green algae, the Mn-cluster is shielded on the luminal side of the thylakoid membrane by the extrinsic proteins PSBO,

PSBP, and PSBQ, with apparent molecular masses of 33, 23, and 17 kDa, respectively (reviewed by Ifuku and Noguchi 2016, Roose *et al.* 2016). These proteins stabilize the Mn-cluster and optimize oxygen evolution by regulating the access and retention of Ca^{2+} and Cl^- (Vinyard and Brudvig 2017). The extrinsic OEC subunits also protect the Mn-cluster from reductants (Popelkova

Highlights

- Microfluidics enables measuring the photosynthetic activity of single cells for days
- Assessment of the lifetime of PSBO became possible with high-time resolution
- PSBO lifetime varies by a factor of 10, depending on light and carbon availability

Received 14 June 2023

Accepted 11 July 2023

Published online 31 July 2023

[†]Corresponding author

e-mail: toth.szilvia@brc.hu

Abbreviations: amiRNA – artificial microRNA; Chl – chlorophyll; *EV31* – empty vector control strain #31; F_0 – minimal fluorescence yield of the dark-adapted state; F_m – maximal fluorescence yield of the dark-adapted state; F_v/F_m – Chl *a* fluorescence parameter, reflecting photosynthetic integrity; OEC – oxygen-evolving complex; PSBO – 33 kD OEC extrinsic protein; TAP – Tris-acetate-phosphate medium; TP – Tris-phosphate medium.

Acknowledgments: This work was supported by the Lendület/Momentum Programme of the Hungarian Academy of Sciences (LP-2014/19), the Alexander von Humboldt Foundation, the National Research, Development and Innovation Office (K132600, GINOP-2.3.2-15-2016-00026, FK135633), and the Eötvös Loránd Research Network (SA-109). We thank Dr. Péter Galajda (BRC, Szeged) for the critical reading of the manuscript and for providing the microfluidic infrastructure.

Conflict of interest: The authors declare that they have no conflict of interest.

et al. 2011, Bricker *et al.* 2012), including luminal ascorbate (Podmaniczki *et al.* 2021). The major subunit, PSBO, may also regulate the access of water to the Mn-cluster and proton removal *via* a hydrogen-bond network (Ho and Styring 2008, Offenbacher *et al.* 2013).

Due to its crucial role in photosynthetic oxygen evolution, PSBO is essential in vascular plants and for the photoautotrophic growth of algae (Mayfield *et al.* 1987, Liu *et al.* 2009, Pigolev and Klimov 2015). In *Arabidopsis thaliana*, PSBO has two isoforms. T-DNA knockout mutants of PSBO1 (*psbo1*) exhibit malfunction on both the donor and acceptor sides of PSII, high susceptibility to photoinhibition, and a severe growth phenotype (Allahverdiyeva *et al.* 2009). On the other hand, the absence of PSBO2 hardly affects PSII activity and plant growth (Lundin *et al.* 2007, Allahverdiyeva *et al.* 2009). In the green alga, *Chlamydomonas reinhardtii*, PSBO is encoded by a single gene (*Cre09.g396213*), and it is indispensable for oxygen evolution (Mayfield *et al.* 1987, Pigolev and Klimov 2015).

PSBO is relatively stable *in vitro* (Hashimoto *et al.* 1996). However, by employing nitrate-inducible PSBO artificial microRNA (amiRNA) lines, we showed that in *C. reinhardtii* PSBO has a significant turnover that is dependent on light intensity and carbon availability (Vidal-Meireles *et al.* 2023). Here, we aimed to obtain more specific data with improved time resolution on the lifetime of PSBO. To this end, we employed single-cell microfluidics. Microfluidic systems enable studying individual cells in a well-defined environment, *in situ* and in real time (e.g., Kim *et al.* 2007, Barber and Emerson 2008, Song *et al.* 2020). Microfluidic technology is also suitable for precisely exchanging culture media without centrifugation or other treatments that may represent stress effects for the algal cells. Recently, we developed the so-called ‘Tulip’ microfluidics platform to capture and immobilize individual *C. reinhardtii* cells without binding them to a solid support surface (Széles *et al.* 2022); our system also enables the long-term measurement of the photosynthetic activity of single cells *via* chlorophyll (Chl) *a* fluorescence (Széles *et al.* 2022).

Materials and methods

Algal strains and growth conditions of bulk cultures: A nitrate-inducible *PSBO* amiRNA transformant, *PSBO-A58*, and its empty vector control *EV31* were used (Vidal-Meireles *et al.* 2023). The *PSBO* amiRNA transformant contains a *NIT1* promoter that drives the expression of the *PSBO* amiRNA construct; it is induced upon changing the nitrogen source from ammonium to nitrate in the growth medium (Schmollinger *et al.* 2010).

Cultures were grown in 50-ml Erlenmeyer flasks for three days in Tris-acetate-phosphate (TAP) medium at 22°C and 80 $\mu\text{mol}(\text{photon}) \text{ m}^{-2} \text{ s}^{-1}$, and they were supplemented with 1.87 mM NH₄Cl₂ on day two of culturing to prevent unwanted induction of the *PSBO* amiRNA construct. For the induction in bulk cultures, cells were washed four times with nitrogen-free Tris-phosphate

(TP) medium and transferred to nitrate-containing (7.48 mM) TAP or TP medium in 250-ml Erlenmeyer flasks. The Chl (*a+b*) content was set to 5 $\mu\text{g} \text{ mL}^{-1}$, determined according to Porra *et al.* (1989).

Chlorophyll *a* fluorescence measurements on bulk cultures: Chlorophyll *a* fluorescence measurements were performed as described in Nagy *et al.* (2018). Briefly, *C. reinhardtii* cultures were dark-adapted for about 15 min, and then 3 ml of cell suspension was filtered onto a *Whatman* glass microfibre filter (GF/B) and measured with a *Handy PEA* instrument (*Hansatech Instruments Ltd.*, UK).

Immunoblot analysis of PSBO: Sample collection was performed as described by Vidal-Meireles *et al.* (2023). Protein separation and Western blotting were carried out as described by Podmaniczki *et al.* (2021). A specific polyclonal antibody against PSBO was purchased from *Agrisera AB* (AS 06 142-33).

Construction and operation of the ‘Tulip’ microfluidic device: The microfluidic device was constructed using standard photolithography and soft lithography techniques (Whitesides *et al.* 2001). The ‘Tulip’ microfluidic device was designed in *KLayout*, an open-source software (www.klayout.de), and it was made of polydimethylsiloxane (*Sylgard 184*, *Dow Corning*), as described in Széles *et al.* (2022).

Liquid cell cultures and solutions were introduced into the microfluidic chips *via* tubing plugged into the inlet holes of the microfluidic device. Fluid flow was ensured and controlled by syringe pumps (*New Era Pump Systems Inc.*, *Model No. 4000*).

The fluid flow properties within the microfluidic device were modeled with *Comsol Multiphysics 4.3a* software. The velocity magnitude profiles were calculated by the ‘Laminar flow’ model. We applied a ‘Shallow channel’ approximation to get a quasi-3D model of the streamlines. The ‘Tulip’ device consists of three parallel channels that were taken into account when building the flow model. We used a 26.7 $\mu\text{l h}^{-1}$ flow rate in the calculations.

Cell loading and culturing in microfluidic devices: The pre-cultures of *EV31* and *PSBO-A58* were grown in 25-ml Erlenmeyer flasks in TAP medium, at 22°C under 80 $\mu\text{mol}(\text{photon}) \text{ m}^{-2} \text{ s}^{-1}$ for three days. Using the pre-culture as an inoculum, a ‘main culture’ was grown in TAP medium for three days, under the above-mentioned conditions. The Chl (*a+b*) content was set to 0.1 $\mu\text{g} \text{ mL}^{-1}$, determined according to Porra *et al.* (1989). Both the pre-culture and the ‘main culture’ were supplemented with 1.87 mM NH₄Cl₂ on day two of cultivation.

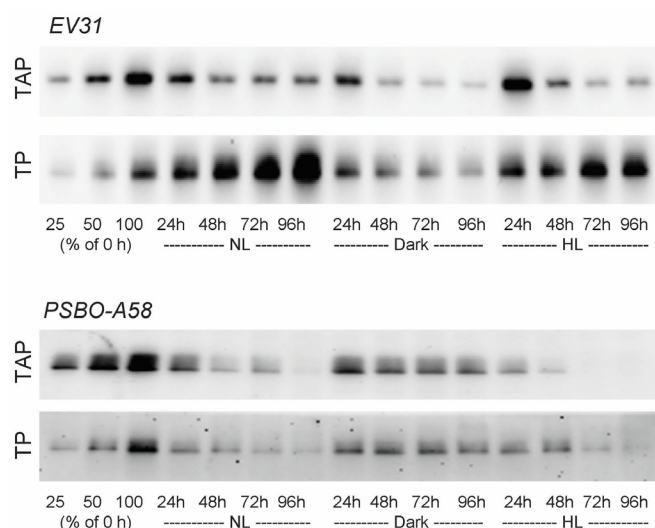
Two separate units of the ‘Tulip’ microfluidic device were loaded with *EV31* and *PSBO* amiRNA cultures of 1 μg Chl (*a+b*) mL^{-1} in TAP medium, at a flow rate of 80 $\mu\text{l h}^{-1}$ for 30 min, ensured by a syringe pump (*New Era Pump Systems Inc.*, *Model No. 4000*). After 30 min, TAP medium was provided, and the flow rate was increased to

360 $\mu\text{l h}^{-1}$ for 4 h. Following that, the TAP medium was swapped with nitrate-containing (7.48 mM) TAP or TP medium at 360 $\mu\text{l h}^{-1}$ flow rate for up to 96 h.

Continuous illumination was provided by white LED spot microscope lamps at an intensity of approx. 90 and 160 $\mu\text{mol}(\text{photon}) \text{m}^{-2} \text{s}^{-1}$ on the surface of the microfluidic device or the cells were kept in the dark during the entire experiment.

Microscopy and Chl *a* fluorescence measurements: The *Microscopy* version of the *Imaging PAM M-series* Chl *a* fluorometer coupled to an *AxioScope A1* microscope (*Zeiss GmbH*) was employed to measure Chl *a* fluorescence using 20 \times and 63 \times objectives (*Zeiss, Fluar 20X/0.75 N.A* and *Zeiss, EC Plan-Neofluar 63X/1.25 N.A*, respectively). The 63 \times oil immersion objective was used for imaging. Bright-field images were captured by an *Axiocam 503* color CCD camera mounted on the microscope with a *60N-C 2/3" 0.63X* video adapter (*Zeiss GmbH*, Jena, Germany).

For Chl *a* fluorescence measurements, the LED light source was equipped with a timer which ensured 15-min dark adaptation before the Chl *a* fluorescence measurement performed every 2nd hour. Chl *a* fluorescence was induced by modulated blue (470 nm) measuring light and the emitted fluorescence image was captured by an *IMAG-K6 CCD* camera (*Walz GmbH*, Germany) mounted on the microscope *via* a *60N-C 2/3" 0.5X* video adapter. To determine the F_0 level of Chl *a* fluorescence, the measuring light intensity was set to level 2 and frequency to 2 Hz – using these settings, the measuring light intensity was not actinic. The gain was set to level 20 and damping to 1 and 5 for 20 \times and 63 \times objectives, respectively. F_m values were obtained by 820-ms saturating blue light pulses at an intensity level of 5. F_v/F_m , a sensitive parameter of PSII integrity, was calculated as $(F_m - F_0)/F_m$. The decay kinetics of F_v/F_m was fitted with a sigmoidal (logistic) function in *Origin (Microcal)* software and the halftime of F_v/F_m diminishment was determined directly from the fitting parameters (XC, the position of inflection points).



Electron microscopy: The ‘Tulip’ microfluidic device was imaged by scanning electron microscopy. For this purpose, the microfluidic devices were coated with a thin layer of gold by a *Quorum Q150T* sputter coater (100 mA, 120 s) and examined with a *JSM-7100F* field emission scanning electron microscope (using 5 kV acceleration voltage).

Statistical analysis: The presented data are based on at least three independent experiments. When applicable, averages and \pm SE were calculated. The significance of the mean differences between the F_v/F_m values of bulk cultures of the *PSBO* amiRNA transformant and the *EV31* strain was analyzed by *Student's t*-test using *GraphPad Prism5* software, and the significance levels are presented when applicable.

Results

Experiments on bulk PSBO amiRNA transformants: Each protein in a living cell has a certain lifetime ranging from minutes to weeks or even years. After this period, in a process called protein turnover, proteins are degraded and replaced by newly synthesized ones. Regarding the functionality of the photosynthetic electron transport chain, the lifetime of PSBO is particularly relevant, since it is an essential subunit of OEC (e.g., *Mayfield et al. 1987*).

To study PSBO lifetime, we used a nitrate-inducible amiRNA line targeting *PSBO*, called *PSBO-A58*, characterized in our recent work (*Vidal-Meireles et al. 2023*). The *PSBO-A58* amiRNA transformant had an equal PSBO level under noninducing conditions as the *EV31* control strain (*Vidal-Meireles et al. 2023*). Under inducing conditions, *i.e.*, upon transferring the cultures from ammonia-containing to nitrate-containing TAP media, the amount of PSBO decreased slowly in the dark, more rapidly at normal light [approx. 100 $\mu\text{mol}(\text{photon}) \text{m}^{-2} \text{s}^{-1}$], and at a particularly high rate at high light [approx. 530 $\mu\text{mol}(\text{photon}) \text{m}^{-2} \text{s}^{-1}$] (Fig. 1). We also observed that in TP medium without carbon supply, the PSBO levels diminish more slowly than that in TAP medium (Fig. 1) or in TP medium with CO₂ supplementation (*Vidal-Meireles*

Fig. 1. Representative immunoblots to monitor the changes in PSBO levels in the empty vector *EV31* strain and the nitrate-inducible *PSBO-A58* amiRNA transformant in the nitrate-containing TAP and TP medium (*i.e.*, without acetate or other carbon supply). The induction was performed on bulk cultures at normal light [100 $\mu\text{mol}(\text{photon}) \text{m}^{-2} \text{s}^{-1}$, NL], in the dark (D), and at high light [530 $\mu\text{mol}(\text{photon}) \text{m}^{-2} \text{s}^{-1}$, HL]. The samples were loaded based on equal cell numbers. The 0 h samples represent the noninduced controls, with cell numbers of 25, 50, and 100%.

et al. 2023). On the other hand, we found that the relative *PSBO* amiRNA transcript abundance was equal, and the *PSBO* transcript level strongly diminished in all growth conditions (Vidal-Meireles *et al.* 2023). This means that the induction of the *PSBO* amiRNA construct was effective, irrespective of light intensity and carbon supply.

PSBO is essential to maintain OEC activity in green algae, and its loss entails donor-side induced photoinhibition in the light (Chen *et al.* 1995, Jegerschöld and Styring 1996), resulting in a substantial diminishment of the F_v/F_m value, a sensitive parameter of PSII integrity (Tóth *et al.* 2011, Vidal-Meireles *et al.* 2023). Donor-side induced photoinhibition is a fast process, occurring on a timescale of a few minutes; therefore, the F_v/F_m value is suitable for tracking the loss of *PSBO* in *C. reinhardtii*. Under noninducing conditions (*i.e.*, at time 0, Fig. 2), the F_v/F_m value was equal in the *PSBO-A58* and the *EV31* strains. In nitrate-containing TAP medium, the F_v/F_m value remained relatively high in the *EV31* strain (Fig. 2A), whereas in the *PSBO-A58* strain, it decreased severely (Fig. 2B), in parallel with the decline of the *PSBO* level (Fig. 1). In nitrate-containing TP medium, the F_v/F_m remained in the *EV31* strain (Fig. 2C), and it declined in the *PSBO-A58* strain albeit much more slowly than in nitrate-TAP (Fig. 2D). We also observed a clear light intensity dependence of the diminishment of *PSBO* (Fig. 2), in agreement with the immunoblot data (Fig. 1, *see also* Vidal-Meireles *et al.* 2023).

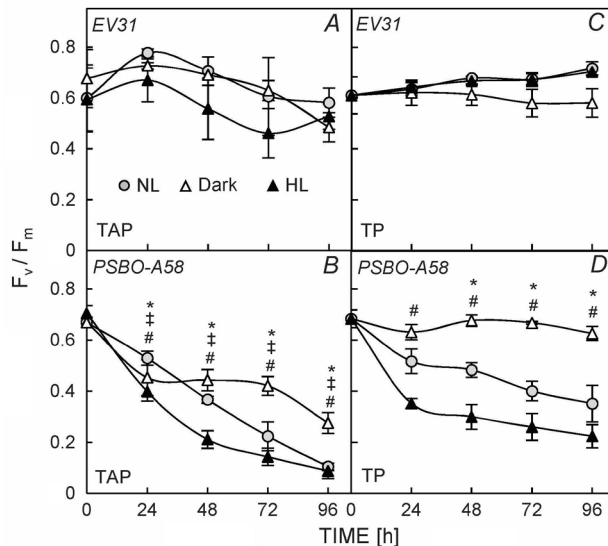


Fig. 2. The effects of downregulating *PSBO* on photosynthesis in bulk cultures, as assessed by the F_v/F_m Chl *a* fluorescence parameter, in the nitrate-inducible *PSBO-A58* amiRNA transformant and the empty vector *EV31* strain in the nitrate-containing TAP and TP medium. The induction was performed on bulk cultures at normal light [$100 \mu\text{mol}(\text{photon}) \text{ m}^{-2} \text{ s}^{-1}$, NL], in the dark (D), and at high light [$530 \mu\text{mol}(\text{photon}) \text{ m}^{-2} \text{ s}^{-1}$, HL]. Values are means \pm SE of four biological replicates. Statistical significance levels are presented relative to the 0 h time point of each sample, as *; ‡; # for the NL, D, and HL samples, respectively, $p < 0.05$.

Induction of the *PSBO* amiRNA transformants in the ‘Tulip’ microfluidics device: The above data demonstrate that *PSBO* lifetime is light-dependent and largely affected by carbon availability. To study *PSBO* lifetime with high-time resolution and precision, we employed single-cell microfluidics in combination with Chl *a* fluorescence measurement.

Our ‘Tulip’ microfluidics platform is suitable for trapping and immobilizing individual cells for several hours (Széles *et al.* 2022). Within the device, the traps are arranged in rows that are laterally shifted with respect to each other (Fig. 3A). The traps have a relatively wide opening (about 28 μm), a narrow middle section (about 8 μm), and an even narrower exit (about 3 μm) to prevent cells from escaping (Fig. 3B). The traps are relatively shallow (about 7 μm) to limit cell movement in the vertical direction thereby improving Chl *a* fluorescence imaging quality.

Computational modeling of the flow field demonstrates that in the case of empty traps, the magnitude of the flow velocity is about 6–7-fold lower at the entrance of the trap compared to the velocity between neighboring traps, and it is the highest at the narrow exits of individual traps (Fig. 3C). Moreover, upon trapping a cell, the flow

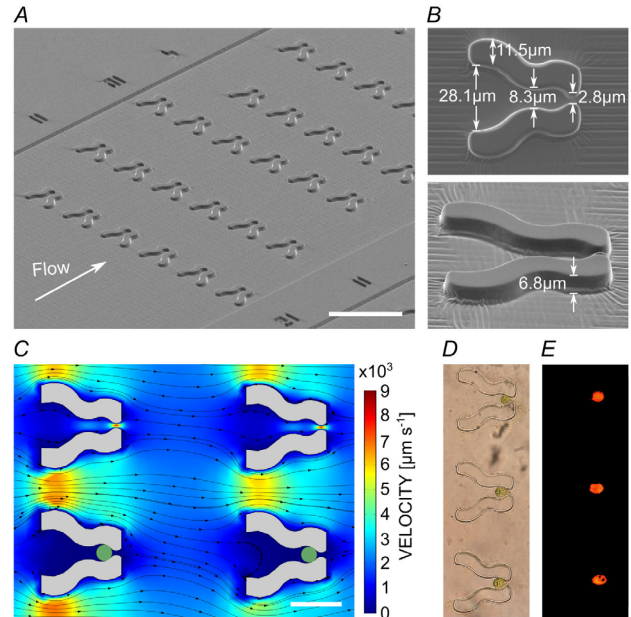


Fig. 3. ‘Tulip’ microfluidics platform for capturing and immobilizing single *C. reinhardtii* cells enabling the measurement of their photosynthetic activity. (A) Scanning electron microscopy image of the device with the direction of media flow indicated by the arrow. Scale bar is 100 μm . (B) Scanning electron microscopy images of single ‘Tulip’ traps from above and at a tilted angle (60°). The approximate characteristic sizes of the traps are shown. (C) Computational modeling of media flow in the device without (upper line) and with cells trapped inside (lower row). The density of the streamlines and the color code represent the velocity magnitude (the scale bar is shown on the right, 30 μm). (D) Representative bright-field microscopy image of trapped *C. reinhardtii* cells. (E) Maximum Chl *a* fluorescence (F_m) values of the captured cells in the ‘Tulip’ device.

is diminished, reducing the chance of another cell entering the trap (Fig. 3C). By holding the cells in their middle sections, the traps act as a physical constraint (Fig. 3C,D), enabling the measurement of photosynthetic parameters on a single cell level (Fig. 3E; Széles *et al.* 2022).

To investigate the lifetime of PSBO, nitrate-inducible *PSBO* amiRNA lines were introduced into the ‘Tulip’ microfluidic device. They were adapted to the new conditions for 4 h; following this stage, the culture media were exchanged from ammonia-containing (regular) TAP to nitrate-containing TAP medium. To investigate the dependence of PSBO lifetime on carbon availability, a nitrate-containing TP medium was used in a set of experiments.

The light dependence of PSBO lifetime was investigated under three conditions: darkness, 90 and 160 $\mu\text{mol}(\text{photon}) \text{ m}^{-2} \text{ s}^{-1}$ of white light. We note that these light intensities were measured on the surface of the microfluidic device, *i.e.*, each cell receives this illumination continuously and uniformly during the entire course of the experiment.

In the dark, the F_v/F_m values of the *PSBO-A58* line decreased continuously in TAP medium and reached a 0 value by the 48th h of induction, with a halftime of about 24.7 h. In the TP medium, the diminishment of F_v/F_m , indicating PSBO loss, was about two-fold slower, occurring with a halftime of about 53 h (Fig. 4A).

In the presence of light, the diminishment of F_v/F_m was remarkably faster: in the TAP medium at 90 $\mu\text{mol}(\text{photon}) \text{ m}^{-2} \text{ s}^{-1}$, it occurred with a halftime of about 12.5 h, whereas in the carbon limitation (TP medium), the halftime was more than double, approx. 30 h (Fig. 4B).

At 160 $\mu\text{mol}(\text{photon}) \text{ m}^{-2} \text{ s}^{-1}$, the diminishment of F_v/F_m was further accelerated, and it reached a 0 value already after 24 h of illumination in the TAP medium, with a halftime of only 5 h. In the TP medium, the diminishment was four-fold slower, occurring with a halftime of about 20 h (Fig. 4C).

The above data show that the induction of the *PSBO-A58* line resulted in a very severe loss of photosynthetic activity. This was accompanied by morphological changes as well, as shown in Fig. 5; after 16 h of induction at 160 $\mu\text{mol}(\text{photon}) \text{ m}^{-2} \text{ s}^{-1}$ in the TAP medium, the cell ultrastructure was severely altered, also substantially affecting the F_0 and F_m images.

Discussion

Most studies on algal physiology have been performed on bulk cultures. The obtained parameters originate from heterogeneous cell populations, in which the individual cells may be in various cell cycle phases and each cell is subjected to continuously changing light conditions as the culture is being stirred. Microfluidics offers an attractive alternative to conventional methods of cultivating individual cells in a well-defined environment. The microfluidic technology also enables the precise control of the cellular microenvironment, including rapid and gentle media exchange; this is a notable advantage

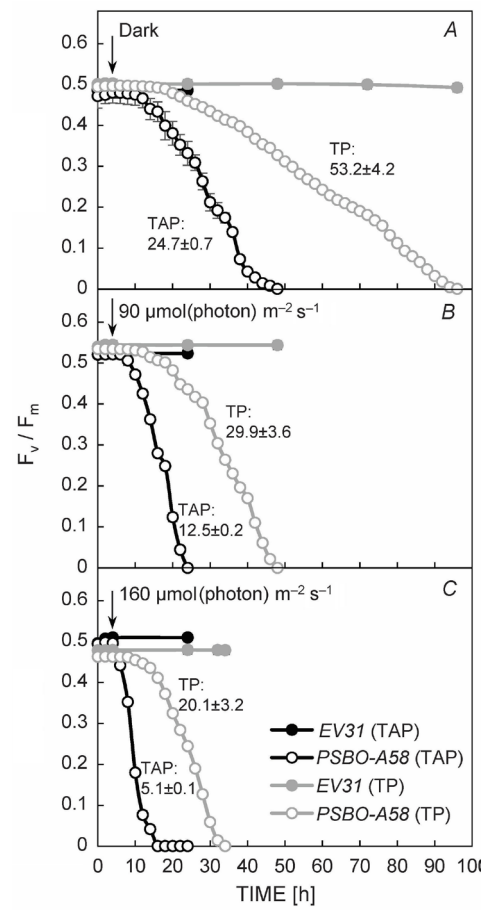


Fig. 4. The effects of downregulating *PSBO* on photosynthesis as assessed by the F_v/F_m parameter, in the nitrate-inducible *PSBO-A58* amiRNA transformant and the empty vector *EV31* strain in the nitrate-containing TAP and TP medium. The induction was performed in the ‘Tulip’ microfluidic device, in the dark (A), at normal light [90 $\mu\text{mol}(\text{photon}) \text{ m}^{-2} \text{ s}^{-1}$, B], and at high light [160 $\mu\text{mol}(\text{photon}) \text{ m}^{-2} \text{ s}^{-1}$, C]. Values are means \pm SE of four biological replicates. The arrows indicate the start of the induction, *i.e.*, the time point of replacing the culture media with the nitrate-containing TAP or TP media. The kinetics were fitted with a Logistic equation, and the X_C values, used to estimate the halftime of F_v/F_m diminishment are displayed in the panels together with the SE of the four independent experiments.

compared to bulk cultures, in which changing the culture media includes centrifugation, inferring stress effects for the cells.

Our microfluidics platform enables constant and stable exposure of individual cells to the given light intensity. Another major advantage is that the same cells can be monitored on the timescale of days. Moreover, the combination with Chl *a* fluorescence enables measuring photosynthetic parameters at high-time resolution and *in situ*. In conventional bulk cultures, determining the changes in photosynthetic activity requires frequent sampling, which could substantially affect the culture parameters. Our system is also automated, so the

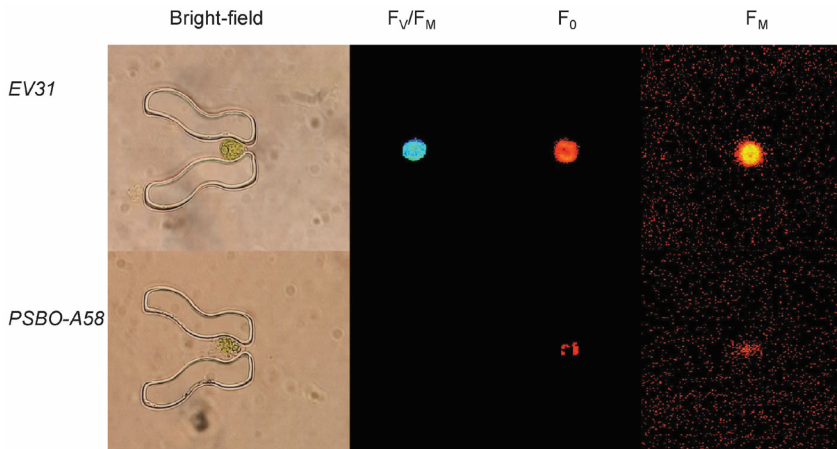


Fig. 5. Representative bright-field microscopy images, F_v/F_m , F_0 , and F_m images of *PSBO-A58* amiRNA transformant and *EV31* cells in the nitrate-containing TAP medium after 16 h of induction at $160 \mu\text{mol}(\text{photon}) \text{m}^{-2} \text{s}^{-1}$ in the 'Tulip' microfluidics device.

measurements can be taken continuously for days, without human intervention.

Using nitrate-inducible amiRNA lines targeting the *PSBO* mRNA, we previously demonstrated that the lifetime of PSBO in *C. reinhardtii* is dependent on both light intensity and carbon source availability (Vidal-Meireles *et al.* 2023). Under noninducing conditions, our nitrate-inducible *PSBO* amiRNA transformants grow normally, and their photosynthetic activity is similar to that of the control strain. Upon induction of amiRNA expression, the cellular PSBO level diminishes, cell division is halted, and the Chl (*a+b*) content decreases (Vidal-Meireles *et al.* 2023). The arrest of cell division and the gradual decline in cellular PSBO content mean that PSBO has significant turnover. In Vidal-Meireles *et al.* (2023), bulk cultures were used, with a few sampling points to avoid changing culture parameters considerably. Therefore, the time course of the diminishment of PSBO level and photosynthetic activity consisted only of a few data points serving as a qualitative descriptor of PSBO lifetime (see also Figs. 1 and 2).

Here, with microfluidics combined with Chl *a* fluorescence-induction measurements, we could obtain high-resolution data on the decline of photosynthetic activity, reflecting the loss of PSBO. This approach is based on the fact that PSBO is essential for the biogenesis and stability of OEC (Liu *et al.* 2009, Piglev and Klimov 2015); the diminishment of OEC activity results in a prompt decrease in F_v/F_m , and the rapidly occurring donor-side-induced photoinhibition further diminishes F_v/F_m (Tóth *et al.* 2011). Indeed, our data presented in this study (Figs. 1, 2) and our previous paper (Vidal-Meireles *et al.* 2023) show that the loss of PSBO and the decline of F_v/F_m occur in parallel in the inducible *PSBO* amiRNA lines.

We found that the diminishment of F_v/F_m in the TAP medium and $90 \mu\text{mol}(\text{photon}) \text{m}^{-2} \text{s}^{-1}$ occurs with halftime of about 12.5 h. By increasing the light intensity to $160 \mu\text{mol}(\text{photon}) \text{m}^{-2} \text{s}^{-1}$, the diminishment of F_v/F_m became remarkably faster, occurring with halftime of about 5 h. In the dark, the F_v/F_m value decreased slowly, with halftime of about 25 h (Fig. 4).

On the other hand, keeping the cells in the TP medium (*i.e.*, carbon-limited conditions) doubled to quadrupled the lifetime of PSBO relative to the TAP medium: at $90 \mu\text{mol}(\text{photon}) \text{m}^{-2} \text{s}^{-1}$, the F_v/F_m value diminished with halftime of about 30 h, whereas at $160 \mu\text{mol}(\text{photon}) \text{m}^{-2} \text{s}^{-1}$, the halftime was about 20 h. In the dark, the diminishment of F_v/F_m occurred very slowly, with halftime of about 53 h.

We noted that the rate of the F_v/F_m diminishment is much faster in our microfluidic device than in bulk cultures (*cf.* Figs. 2 and 4); the reason may be that in the microfluidic device each cell is exposed continuously to the same, constant light intensity, and the cells do not shade each other. On the other hand, it is also conceivable that the exchange of culture media from the ammonium-containing to nitrate-containing ones occurs more effectively, therefore, the induction of the amiRNA construct is also faster.

Thus we could show that under photoautotrophic conditions (*i.e.*, in the TP medium), the cellular PSBO content is at least two-fold more stable in comparison with acetate-supplied cultures (Fig. 4). Acetate mitigates singlet oxygen production in *C. reinhardtii* (Roach *et al.* 2013) and excess acetate reduces the rates of CO_2 fixation and oxygen evolution without affecting PSII integrity (Heifetz *et al.* 2000), thus it is unlikely that acetate itself led to PSBO damage. Moreover, we found earlier that CO_2 supplementation also decreases the lifetime of PSBO (Vidal-Meireles *et al.* 2023), showing that PSBO lifetime in *C. reinhardtii* largely depends on carbon availability. This may be related to the fact that carbon-limited cultures are metabolically less active, which, similarly to yeast and mammals subjected to nutrient limitation, leads to lifespan prolongation (López-Otín *et al.* 2016, Sampaio-Marques *et al.* 2019, Zamzam *et al.* 2022).

Biomass accumulation can be limited in various biotechnological applications of green algae, such as in biofilm culturing systems (*e.g.*, Vajravel *et al.* 2020), and bio-hydrogen production platforms with restricted carbon assimilation (Kosourov *et al.* 2018, Nagy *et al.* 2021). Due to the high cost of establishing new algal cultures, they must be maintained for a long period to be remunerative.

Therefore, determining the lifetimes of photosynthetic subunits is highly relevant for the bio-industry. Our findings on PSBO lifetime suggest that the photosynthetic activity can be better maintained in moderate light and with a limited carbon supply.

References

Allahverdiyeva Y., Mamedov F., Holmström M. *et al.*: Comparison of the electron transport properties of the *psb01* and *psb02* mutants of *Arabidopsis thaliana*. – BBA-Bioenergetics **1787**: 1230-1237, 2009.

Barber R.W., Emerson D.R.: Optimal design of microfluidic networks using biologically inspired principles. – Microfluid. Nanofluid. **4**: 179-191, 2008.

Bricker T.M., Roose J.L., Fagerlund R.D. *et al.*: The extrinsic proteins of Photosystem II. – BBA-Bioenergetics **1817**: 121-142, 2012.

Chen G.-X., Blubaugh D.J., Homann P.H. *et al.*: Superoxide contributes to the rapid inactivation of specific secondary donors of the photosystem II reaction-center during photodamage of manganese-depleted photosystem II membranes. – Biochemistry **34**: 2317-2332, 1995.

Hashimoto A., Yamamoto Y., Theg S.M.: Unassembled subunits of the photosynthetic oxygen-evolving complex present in the thylakoid lumen are long-lived and assembly-competent. – FEBS Lett. **391**: 29-34, 1996.

Heifetz P.B., Förster B., Osmond C.B. *et al.*: Effects of acetate on facultative autotrophy in *Chlamydomonas reinhardtii* assessed by photosynthetic measurements and stable isotope analyses. – Plant Physiol. **122**: 1439-1446, 2000.

Ho F.M., Styring S.: Access channels and methanol binding site to the CaMn₄-cluster in photosystem II based on solvent accessibility simulations, with implications for substrate water access. – BBA-Bioenergetics **1777**: 140-153, 2008.

Ifuku K., Noguchi T.: Structural coupling of extrinsic proteins with the oxygen-evolving center in photosystem II. – Front. Plant Sci. **7**: 84, 2016.

Jegerschöld C., Styring S.: Spectroscopic characterization of intermediate steps involved in donor-side-induced photoinhibition of photosystem II. – Biochemistry **35**: 7794-7801, 1996.

Kim L., Toh Y., Voldman J., Yu H.: A practical guide to microfluidic perfusion culture of adherent mammalian cells. – Lab Chip **7**: 681-694, 2007.

Kosourov S., Jokel M., Aro E.-M., Allahverdiyeva Y.: A new approach for sustained and efficient H₂ photoproduction by *Chlamydomonas reinhardtii*. – Energy Environ. Sci. **11**: 1431-1436, 2018.

Liu H., Frankel L.K., Bricker T.M.: Functional complementation of the *Arabidopsis thaliana psb01* mutant phenotype with an N-terminally His₆-tagged PsbO-1 protein in photosystem II. – BBA-Bioenergetics **1787**: 1029-1038, 2009.

López-Otín C., Galluzzi L., Freije J.M.P. *et al.*: Metabolic control of longevity. – Cell **166**: 802-821, 2016.

Lundin B., Hansson M., Schoefs B. *et al.*: The *Arabidopsis* PsbO2 protein regulates dephosphorylation and turnover of the photosystem II reaction centre D1 protein. – Plant J. **49**: 528-539, 2007.

Mayfield S., Bennoum P., Rochaix J.-D.: Expression of the nuclear-encoded OEE1 proteins is required for oxygen evolution and stability of photosystem II particles in *Chlamydomonas reinhardtii*. – EMBO J. **6**: 313-318, 1987.

Nagy V., Podmaniczki A., Vidal-Meireles A. *et al.*: Thin cell layer cultures of *Chlamydomonas reinhardtii* L159I-N230Y, *pgr11* and *pgr5* mutants perform enhanced hydrogen production at sunlight intensity. – Bioresource Technol. **333**: 125217, 2021.

Nagy V., Vidal-Meireles A., Podmaniczki A. *et al.*: The mechanism of photosystem-II inactivation during sulphur deprivation-induced H₂ production in *Chlamydomonas reinhardtii*. – Plant J. **94**: 548-561, 2018.

Offenbacher A.R., Polander B.C., Barry B.A.: An intrinsically disordered photosystem II subunit, PsbO, provides a structural template and a sensor of the hydrogen-bonding network in photosynthetic water oxidation. – J. Biol. Chem. **288**: 29056-29068, 2013.

Pigolev A.V., Klimov V.V.: The green alga *Chlamydomonas reinhardtii* as a tool for *in vivo* study of site-directed mutations in PsbO protein of photosystem II. – Biochemistry-Moscow **80**: 662-673, 2015.

Podmaniczki A., Nagy V., Vidal-Meireles A. *et al.*: Ascorbate inactivates the oxygen-evolving complex in prolonged darkness. – Physiol. Plantarum **171**: 232-245, 2021.

Popelkova H., Boswell N., Yocom C.: Probing the topography of the photosystem II oxygen evolving complex: PsbO is required for efficient calcium protection of the manganese cluster against dark-inhibition by an artificial reductant. – Photosynth. Res. **110**: 111-121, 2011.

Porra R.J., Thompson W.A., Kriedemann P.E.: Determination of accurate extinction coefficients and simultaneous equations for essaying chlorophylls *a* and *b* with four different solvents: verification of the concentration of chlorophyll standards by atomic absorption spectroscopy. – BBA-Bioenergetics **975**: 384-394, 1989.

Roach T., Sedoud A., Krieger-Liszkay A.: Acetate in mixotrophic growth medium affects photosystem II in *Chlamydomonas reinhardtii* and protects against photoinhibition. – BBA-Bioenergetics **1827**: 1183-1190, 2013.

Roose J.L., Frankel L.K., Mummadisetti M.P., Bricker T.M.: The extrinsic proteins of photosystem II: update. – Planta **243**: 889-908, 2016.

Sampaio-Marques B., Burhans W.C., Ludovico P.: Yeast at the forefront of research on ageing and age-related diseases. – In: Sá-Correia I. (ed): Yeasts in Biotechnology and Human Health. Progress in Molecular and Subcellular Biology. Vol. 58. Pp. 217-242. Springer, Cham 2019.

Schmollinger S., Strenkert D., Schröder M.: An inducible artificial microRNA system for *Chlamydomonas reinhardtii* confirms a key role for heat shock factor 1 in regulating thermotolerance. – Curr. Genetics **56**: 383-389, 2010.

Song K., Li G., Zu X. *et al.*: The fabrication and application mechanism of microfluidic systems for high throughput biomedical screening: a review. – Micromachines **11**: 297, 2020.

Széles E., Nagy V., Ábrahám Á. *et al.*: Microfluidic platforms designed for morphological and photosynthetic investigations of *Chlamydomonas reinhardtii* on a single-cell level. – Cells **11**: 285, 2022.

Tóth S.Z., Nagy V., Puthur J.T. *et al.*: The physiological role of ascorbate as photosystem II electron donor: protection against photoinactivation in heat-stressed leaves. – Plant Physiol. **156**: 382-392, 2011.

Vajravel S., Sirin S., Kosourov S., Allahverdiyeva Y.: Towards sustainable ethylene production with cyanobacterial artificial biofilms. – Green Chem. **22**: 6404-6414, 2020.

Vidal-Meireles A., Kuntam S., Széles E. *et al.*: The lifetime of the oxygen-evolving complex subunit PSBO depends on light intensity and carbon availability in *Chlamydomonas*. – Plant Cell Environ. **46**: 422-439, 2023.

Vinyard D.J., Brudvig G.W.: Progress toward a molecular mechanism of water oxidation in photosystem II. – Annu.

Rev. Phys. Chem. **68**: 101-116, 2017.
Whitesides G.M., Ostuni E., Takayama S. *et al.*: Soft lithography
in biology and chemistry. – Annu. Rev. Biomed. Eng. **3**: 335-
373, 2001.

Zamzam G., Lee C.W.J., Milne F. *et al.*: Live long and prosper:
Acetate and its effects on longevity in batch culturing of
Chlamydomonas reinhardtii. – Algal Res. **64**: 102676, 2022.

© The authors. This is an open access article distributed under the terms of the Creative Commons BY-NC-ND Licence.